# A symmetric consistent immersed finite element method for elliptic interface problems with nonhomogeneous jump conditions

Haifeng Ji, Qian Zhang
School of Mathematical Sciences,
Jiangsu Key Laboratory for NSLSCS,
Nanjing Normal University, Nanjing 210023, China

**Abstract**

In this paper, we present a symmetric and consistent immersed finite element method on Cartesian meshes for elliptic interface problems with nonhomogeneous jump conditions. The nonhomogeneous immersed finite element space which satisfies the nonhomogeneous jump conditions is constructed and used as the trial function space. For the test function space, we use the standard immersed finite element space which satisfies the homogeneous jump conditions. To cancel the consistent error caused by the discontinuity of the test function, some correction terms are added to the weak form near the interface. Our method can handle the case when the interface passes through grid points or the boundary of the domain. Extensive numerical experiments are presented and show that the new method has optimal convergence in $L^2$, $H^1$ and $L^\infty$ norms.

**keyword**: immersed finite element, interface problems, Cartesian mesh, nonhomogeneous jump conditions, symmetric formulation

**AMS subject classification.** 65N15, 65N30, 35J60

## 1 Introduction

In this paper, we consider the following elliptic interface problem

$$-\nabla \cdot (\beta(\mathbf{x})\nabla u(\mathbf{x})) = f(\mathbf{x}), \qquad \mathbf{x} \in \Omega\backslash\Gamma, \tag{1.1}$$

$$u(\mathbf{x}) = g(\mathbf{x}), \qquad \mathbf{x} \in \partial\Omega, \tag{1.2}$$

together with the nonhomogeneous jump conditions across the interface $\Gamma$

$$[u]_\Gamma(\mathbf{x}) = u^+(\mathbf{x}) - u^-(\mathbf{x}) = w(\mathbf{x}), \qquad \mathbf{x} \in \Gamma, \tag{1.3}$$

$$\left[\beta \frac{\partial u}{\partial \mathbf{n}}\right]_\Gamma (\mathbf{x}) = \beta \nabla u^+ \cdot \mathbf{n} - \beta \nabla u^- \cdot \mathbf{n} = Q(\mathbf{x}), \qquad \mathbf{x} \in \Gamma, \tag{1.4}$$

where $\Omega = \Omega^+ \cup \Omega^- \cup \Gamma$ and $\mathbf{n}$ is outward normal of $\Omega^-$. Here the interface $\Gamma$ may intersect with the boundary $\partial\Omega$. The interface $\Gamma$ is often represented by the zero level set of a smooth function $\varphi(\mathbf{x})$ which is called a level-set function. We assume that $\Omega^- = \{\mathbf{x} \in \Omega : \varphi(\mathbf{x}) < 0\}$ and $\Omega^+ = \{\mathbf{x} \in \Omega : \varphi(\mathbf{x}) > 0\}$, then $\mathbf{n} = \nabla\varphi/|\nabla\varphi|$, see Figure 1 for an illustration. The coefficient $\beta(\mathbf{x})$ is uniformly elliptic and continuously differentiable on each subdomain, $\Omega^+$ and $\Omega^-$, that is, there exist two positive constants $0 < \beta_{\min} \le \beta_{\max} < \infty$ such that

$$\beta_{\min} \le \beta(\mathbf{x}) = \beta^i(\mathbf{x}) \le \beta_{\max} \quad \text{for } \mathbf{x} \in \Omega^i,\ i = \pm. \tag{1.5}$$

This problem appears in many applications, such as fluid mechanics, materials science and biological

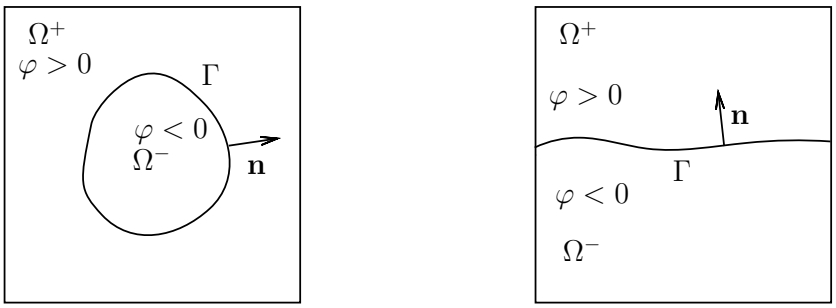


Figure 1: Left: the interface $\Gamma$ lies strictly inside $\Omega$. Right: the interface $\Gamma$ intersects with the boundary $\partial\Omega$.

science. For an example, the static electric potential $u$ satisfies the interface jump conditions (1.3)-(1.4) with $w = 0$ and $Q \neq 0$ on the interface between two media if the surface charge density is not zero.

There are variety of numerical methods proposed in the literature to solve such an interface problem. We refer the reader to [24] for a survey of different numerical methods. It is well known that accurate approximations can be generated by standard finite element methods if the triangulation is aligned with the interface, that is, a body fitted mesh is used, see for example, [1, 4, 31]. However, it may be difficult and time consuming to generate a body fitted mesh for an interface problem in which the interface separates the solution domain into pieces with complicated geometries (especially in 3D). Such a difficulty may become even severer for moving interface problems because a new mesh has to be generated at each time step, or every other time steps. We limit our discussion here to methods on structured meshes that do not align with the interface. The immersed interface method

(IIM) [18, 21] is a second order Cartesian grid method for interface problems. Discontinuities in the solution and the normal gradient at the interface are explicitly incorporated into the finite difference stencil. For problems with sharp edges, the matched interface boundary (MIB) method has been proposed in [34, 33]. Similar to the IIM, the MIB method locally modifies the finite difference stencils near the interface to enforce the interface jump conditions. The resulting linear systems of equations from these methods are nonsymmetric and indefinite even the original problem is self-adjoint and uniformly elliptic.

For finite element methods on structured meshes that do not align with the interface, the immersed finite element method (IFEM) has been developed in [20, 24]. In [24], two types of IFEM were developed: the non-conforming and conforming ones. For the non-conforming IFEM, the basis functions are still piecewise linear but are modified in the elements where the interface cuts through so that the jump conditions are satisfied. While it has been shown that the non-conforming IFEM is second order in the $L^2$ norm [5], it does not have the optimal convergence rate in the $L^\infty$ norm due to the consistent error caused by the discontinuities of the test functions (not in $H^1(\Omega)$ space). The same behavior has also been observed when the method is generalized to the bilinear immersed finite element method [10, 11], to the planar elasticity interface problems [27, 32]. Nevertheless, the non-conforming IFEM has been extensively studied in [5, 23]. Other related works in this direction can be found in [2, 12, 17, 13, 26, 25] and others. Note that, by using the Petrov-Galerkin finite element discretization, the method developed in [14, 15] cancels the consistent error and then achieves second order convergence in the $L^\infty$ norm. But the resulting linear system of equations of the Petrov-Galerkin type method is nonsymmetric because of the different trial and test spaces. We also note that the conforming IFEM proposed in [24] has optimal convergence rate in $L^\infty$ norm and the resulting linear system of equations is symmetric and positive definite. But the basis functions of the conforming IFEM have wider support near the interface and the implementation is non-trivial. Thus the conforming IFEM has not attracted enough interest in the literature. Recently a symmetric and consistent IFEM has been developed in [16]. The method maintains the advantages of the non-conforming IFEM by using the same basis functions but it is symmetric, consistent, and second accurate in $L^\infty$ norm. The idea is to add some correction terms to the weak form to take into account of the discontinuities in basis functions. Other finite elements for interface problems include the extended finite element method (XFEM) in which enrichment functions are added near the interface [7]; unfitted finite element method based on the Nitsche's method[9, 28], and many others. Note that immersed finite volume methods for elliptic interface problems with nonhomogeneous jump conditions has been proposed in [29, 30]. The method has second order convergence in $L^\infty$ norm, but the resulting linear system of equations is also nonsymmetric.

However, most of the previous articles about IFEM are developed for interface problems with the homogeneous jump conditions ($w = 0, Q = 0$). For interface with nonhomogeneous jump conditions, X. He, T. Lin and Y. Lin [11] have developed an IFEM by enriching the IFE spaces locally in interface elements to capture the nonhomogeneous flux jump condition. Note that the case $w \neq 0$ is not considered in that paper. Kwang S. Chang and D. Y. Kwak [3] have proposed a new numerical method to solve an elliptic problem with jumps both in the solution and flux along the interface. A bubble function is constructed to satisfy the same jumps as the exact solution in that paper.

And the method can also handle the case when the interface passes through grid points. Y. Gong, B. Li and Z. Li [8] have developed an IFEM by removing the source singularities caused by the nonhomogeneous interface conditions. Note that a similar technique has been proposed in [6] to solve internal discontinuity interface problems.

It is very important in scientific computing to develop a numerical method which the resulting linear system of equations is symmetric and positive. In this paper, a symmetric and consistent immersed finite element method is proposed for the elliptic interface problem (1.1)-(1.2) with the nonhomogeneous jump conditions. We use the technique introduced in [11, 3] to construct the IFE functions to satisfy the nonhomogeneous jump conditions across the interface. To cancel the consistent error caused by the discontinuity of the test function, some correction terms are added to the bilinear form to preserve the symmetry and consistency. Our method can also handle the case when the interface passes through grid points. Extensive numerical experiments are presented and show that the new method has optimal convergence in $L^2$, $H^1$ and $L^\infty$ norms.

The rest of the paper is organized as follows. In section 2, we introduce the weak form and some notations. In section 3, first we construct two immersed finite element spaces, and then we propose some immersed finite methods. In section 4, we provide various numerical experiments that show the optimal convergence of the new method and compare with other methods. We conclude in section 5.

## 2 Weak formulation

Let $R_\Gamma$ and $R_{\partial\Omega}$ denote the restriction operators from $H^1(\Omega)$ to $L^2(\Gamma)$ and $L^2(\partial\Omega)$, respectively. We assume that boundary data $w$, $Q$ and $g$ are the restrictions of functions $\widetilde{w}$, $\widetilde{Q}$ and $\widetilde{g} \in H^1(\Omega)$, respectively. That is, on $\Gamma$

$$w = R_\Gamma(\widetilde{w}), \qquad Q = R_\Gamma(\widetilde{Q}), \qquad g = R_{\partial\Omega}(\widetilde{g}). \tag{2.1}$$

We also assume that there exist a function $\widetilde{c} \in H^1(\Omega)$ such that

$$g = \begin{cases} R_{\partial\Omega}(\widetilde{c} - \widetilde{w}) & \text{on } \partial\Omega \cap \partial\Omega^-, \\ R_{\partial\Omega}(\widetilde{c}) & \text{on } \partial\Omega \backslash \partial\Omega^-. \end{cases} \tag{2.2}$$

If $\partial\Omega \cap \partial\Omega^- = \emptyset$, i.e. $\Omega^-$ lies strictly inside $\Omega$, then we can chose $\widetilde{c} = \widetilde{g}$. To simplify the notations, from now on we will drop the tildes. For the derivation of the weak formulation, we define the space

$$H(w, c) = \{u : u - c - w\chi_{\Omega^-} \in H_0^1(\Omega)\}, \tag{2.3}$$

in which $\chi_{\Omega^-}$ is the characteristic function of $\Omega^-$. If $u \in H(w, c)$, then $[u]_\Gamma = w$ and $u|_\Omega = g$. Note that $H_0^1(\Omega)$ can be identified with H(0,0).

The original problem (1.1)-(1.4) is equivalent to find $u \in H(w, c)$ such that

$$a(u, v) = \int_\Omega f v d\mathbf{x} - \int_\Gamma Q v ds \qquad \forall v \in H_0^1(\Omega), \tag{2.4}$$

where

$$a(u,v)=\int_{\Omega^-}\beta\nabla u\cdot\nabla v d\mathbf{x}+\int_{\Omega^+}\beta\nabla u\cdot\nabla v d\mathbf{x}.$$

**Theorem 2.1.** *If $f\in L^2(\Omega)$, and $w$, $Q$ and $c\in H^1(\Omega)$, and $\Gamma$ is Lipschitz continuous, then there exist a unique weak solution of (2.4) in $H(w,c)$.*

*Proof.* See [14] for details. □

In traditional Galerkin methods, we usually construct trial function space $U_h(\Omega)$ and test function space $V_h(\Omega)$ to approximate $H(w,c)$ and $H_0^1(\Omega)$ respectively, and then solve the problem (2.4) to get discrete solution $u_h$. If $V_h(\Omega)\notin H_0^1(\Omega)$, then the method has a consistent error, i.e. $a(u-u_h,v_h)\neq 0$, $\forall v_h\in V_h(\Omega)$. Since we use the structured meshes that do not align with the interface, the interface can cut through the inner of elements which are called interface elements. When we construct trial function space $U_h(\Omega)$, we must take account of the jump conditions (1.3)-(1.4) to get a good approximation on these interface elements. The nonhomogeneous IFE space discussed in subsection 3.2.2 is constructed to approximate $H(w,c)$.

# 3 Numerical methods

## 3.1 The mesh

For simplicity of presentation, we assume that $\Omega$ is a rectangular domain. First we partition the domain into a union of uniform rectangles of mesh size $h$. Then we obtain the triangulation $\mathcal{T}_h$ by cutting the rectangles along one of diagonals (in the same direction), see Figure 2. If we choose $h$ sufficiently small, then it is reasonable to assume the following assumption.

- The interface $\Gamma$ will not intersect an edge of any element at more than two points unless this edge is part of $\Gamma$;
- If $\Gamma$ intersects the boundary of a triangular element at two points, then these two points must be on different edges of this element.

Define

$$\begin{aligned}&\mathcal{N}_h=\{\mathbf{x}_i\in\overline{\Omega}:\mathbf{x}_i\text{ is a vertex of a element}\},\\&\mathcal{N}_h^i=\mathcal{N}_h\cap\Omega,\quad \mathcal{N}_h^b=\mathcal{N}_h\cap\partial\Omega,\quad \mathcal{N}_h^s=\mathcal{N}_h\cap\Gamma.\end{aligned}\tag{3.1}$$

The interface $\Gamma$ is approximated by $\Gamma_h$, the union of the line segments connecting the intersections of the interface and the edges of elements. That is

$$\Gamma_h=\bigcup_{i=1}^{M}\Gamma_h^i,\qquad \Gamma_h^i=\overline{\mathbf{x}^i\mathbf{x}^{i+1}},\qquad \mathbf{x}^1=\mathbf{x}^{M+1},\tag{3.2}$$

where $\mathbf{x}^i$ is the intersections of the interface and edges of elements. Such an approximation will not affect second order convergence when $\Gamma \in C^2$, see for example [1, 4].

We call an element $T$ an interface element if $\Gamma$ intersects $\partial T$ at two points; otherwise we call $T$ a non-interface element. The sets of all interface elements and non-interface elements are denoted by $\mathcal{T}_h^{int}$ and $\mathcal{T}_h^{non}$, respectively. To deal with $[u]_\Gamma \neq 0$, we define

$$\mathcal{T}_h^d = \{T \in \mathcal{T}_h^{non} : \ T \subset \Omega^+, \ \Gamma \text{ intersects with } \partial T \text{ at only one vertex}\}. \tag{3.3}$$

Let $\mathcal{E}_h$ be the set of the open edges in $\mathcal{T}_h$. Analogously, we define

$$\mathcal{E}_h^{int} = \{e \in \mathcal{E}_h : e \cap \Gamma \neq \emptyset\}, \tag{3.4}$$

and $\mathcal{E}_h^{non} = \mathcal{E}_h \backslash \mathcal{E}_h^{int}$. An example of the mesh and $\mathcal{T}_h^{int}$, $\mathcal{E}_h^{int}$, $\mathcal{T}_h^d$ is shown in Figure 2.

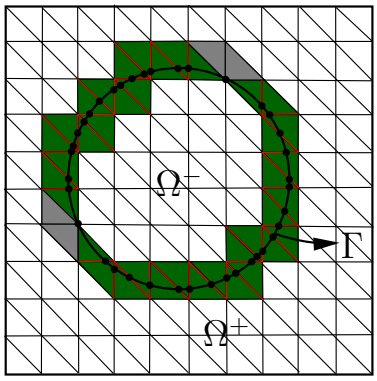


Figure 2: Gray: $\mathcal{T}_h^d$ ; Dark green: $\mathcal{T}_h^{int}$; Red: $\mathcal{E}_h^{int}$.

## 3.2 Immersed finite element spaces

On a non-interface element $T \in \mathcal{T}_h^{non}$, we use the standard linear finite element, and the local base functions associated with the vertices of $T$ are denoted by $\phi_{i,T}$, $i = 1, 2, 3$.

On an interface element $T \in \mathcal{T}_h^{int}$, we use the following typical element to describe the IFE base functions. Let $A(x_1^A, x_2^A)$, $B(x_1^B, x_2^B)$, and $C(x_1^C, x_2^C)$ be vertices of interface element $\triangle ABC$, and $D(x_1^D, x_2^D)$ and $E(x_1^E, x_2^E)$ be the intersections of the interface $\Gamma$ and $\partial T$, see the illustration in Figure 3. The line $\overline{DE}$ separates $T$ into two sub-elements $T^+$ and $T^-$. Let $\mathbf{n}$ be unit vector perpendicular to the line $\overline{DE}$. To construct a interpolation function for approximating the exact solution satisfying the interface jump conditions, we define the following piecewise linear functions on the element $T$

$$\phi(\mathbf{x}) = \begin{cases} \phi^+ = a^+ + b^+ x_1 + c^+ x_2, & \mathbf{x} = (x_1, x_2) \in T^+, \\ \phi^- = a^- + b^- x_1 + c^- x_2, & \mathbf{x} = (x_1, x_2) \in T^-, \end{cases} \tag{3.5}$$

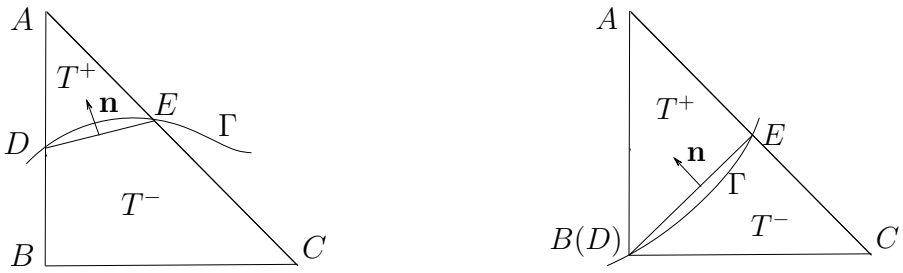


Figure 3: Two typical interface elements.

satisfying

$$\phi(x_1^A, x_2^A) = V_1,\ \phi(x_1^B, x_2^B) = V_2,\ \phi(x_1^C, x_2^C) = V_3, \tag{3.6}$$

$$\phi^+(x_1^D, x_2^D) - \phi^-(x_1^D, x_2^D) = V_4, \tag{3.7}$$

$$\phi^+(x_1^E, x_2^E) - \phi^-(x_1^E, x_2^E) = V_5, \tag{3.8}$$

$$\widetilde{\beta}^+ \nabla\phi^+ \cdot \mathbf{n} - \widetilde{\beta}^- \nabla\phi^- \cdot \mathbf{n} = V_6 \tag{3.9}$$

where $\widetilde{\beta}^+ = \frac{\beta^+(x_1^D, x_2^D) + \beta^+(x_1^E, x_2^E)}{2}$ and $\widetilde{\beta}^- = \frac{\beta^-(x_1^D, x_2^D) + \beta^-(x_1^E, x_2^E)}{2}$. Specifically, (3.5)-(3.9) leads to the following algebraic system for determining the uncertain coefficients,

$$\mathbf{MC} = \mathbf{V},\ \mathbf{C} = (a^+, b^+, c^+, a^-, b^-, c^-)^T,\ \mathbf{V} = (V_1, V_2, V_3, V_4, V_5, V_6)^T, \tag{3.10}$$

where

$$\mathbf{M} = \begin{pmatrix} x_1^A & x_2^A & 1 & 0 & 0 & 0 \\ 0 & 0 & 0 & x_1^B & x_2^B & 1 \\ 0 & 0 & 0 & x_1^C & x_2^C & 1 \\ x_1^D & x_2^D & 1 & -x_1^D & -x_2^D & -1 \\ x_1^E & x_2^E & 1 & -x_1^E & -x_2^E & -1 \\ n_1\widetilde{\beta^+} & n_2\widetilde{\beta^+} & 0 & -n_1\widetilde{\beta^-} & -n_2\widetilde{\beta^-} & 0 \end{pmatrix}, \tag{3.11}$$

with $\mathbf{n} = (n_1, n_2)^T$.

**Remark 3.1.**
*1. The interface $\Gamma$ may intersect with the vertex of the interface element $T$, see 3(b). In this case, $D$ coincide with $B$. Because $w \neq 0$, $\phi(x_1^B, x_2^B)$ has two distinct values. We restrict it on $\Omega^-$, that is $\phi(x_1^B, x_2^B) = \phi^-(x_1^B, x_2^B) = V_2$ in (3.6).*
*2. The matrix $\mathbf{M}$ is invertible, see [24, 23, 22].*

The interpolation of exact solution $u$ on the interface element $T = \triangle ABC$ is

$$(I_h u)_T(\mathbf{x}) = \begin{cases} (1, x_1, x_2, 0, 0, 0)\mathbf{M}^{-1}\mathbf{V} & \mathbf{x} = (x_1, x_2) \in T^+, \\ (0, 0, 0, 1, x_1, x_2)\mathbf{M}^{-1}\mathbf{V} & \mathbf{x} = (x_1, x_2) \in T^-, \end{cases} \tag{3.12}$$

where

$$\mathbf{V} = (u(x_1^A, x_2^A), u(x_1^B, x_2^B), u(x_1^C, x_2^C), w(x_1^D, x_2^D), w(x_1^E, x_2^E), \frac{Q(x_1^D, x_2^D) + Q(x_1^E, x_2^E)}{2})^T. \quad (3.13)$$

If we notice that the vector $\mathbf{V}$ can expressed as $\mathbf{V} = u(x_1^A, x_2^A)\mathbf{e}_1 + u(x_1^B, x_2^B)\mathbf{e}_2 + u(x_1^C, x_2^C)\mathbf{e}_3 + \mathbf{V^J}$, where $\mathbf{V^J} = \left(0, 0, 0, w(x_1^D, x_2^D), w(x_1^E, x_2^E), \frac{Q(x_1^D, x_2^D) + Q(x_1^E, x_2^E)}{2}\right)^T$, then $(I_h u)_T = u(x_1^A, x_2^A)\phi_{A,T} + u(x_1^B, x_2^B)\phi_{B,T} + u(x_1^C, x_2^C)\phi_{C,T} + \phi_{J,T}$. The functions $\phi_{A,T}$, $\phi_{B,T}$, $\phi_{C,T}$ and $\phi_{J,T}$ are defined in the following subsections and are used to construct two IFE spaces.

### 3.2.1 Homogeneous IFE space

Using $\mathbf{V} = \mathbf{e}_i \in R^6$, $1 \le i \le 3$, we can solve (3.10) for $\mathbf{C}$ and use them in (3.5) to obtain the $i$-th IFE nodal local basis function $\phi_{i,T}$, $1 \le i \le 3$. We note that $\phi_{i,T}$ satisfies homogeneous interface jump conditions.

To get the global base functions, we define $R(i, T) = j$, where the global node number $j$ relates the local node number, $i$, on a element $T \in \mathcal{T}_h$. Then the $j$-th global base function $\phi_j$, $j \in \mathcal{N}$ is

$$\phi_j = \sum_{R(i,T)=j} \phi_{i,T}. \quad (3.14)$$

Then we define the IFE space $S_{h0}(\Omega) = \text{span}\{\phi_j, j \in \mathcal{N}^i\}$, which satisfying homogeneous interface jump conditions and homogeneous boundary condition. We must point out that $S_{h0} \not\in H_0^1(\Omega)$ because of the discontinuity on $e \in \mathcal{E}_h^{int}$, see [24].

### 3.2.2 Nonhomogeneous IFE space

Using $\mathbf{V} = \mathbf{V^J}$, we can solve (3.10) for $\mathbf{C}$ and use them in (3.5) to obtain the function $\phi_{J,T}$. We note that $\phi_{J,T}$ satisfies the non-homogeneous jump conditions and the values of vertices of $T$ are zeros. Then we define the following function to capture the nonhomogeneous jump conditions and the boundary condition,

$$u_J = \sum_{T \in \mathcal{T}_h^{int}} \phi_{J,T} + \sum_{\mathbf{x}_j \in \mathcal{N}^s} \sum_{R(i,T)=j, T \in \mathcal{T}_h^d} \phi_{i,T} + \sum_{\mathbf{x}_j \in \mathcal{N}_h^b} \sum_{R(i,T)=j} g(\mathbf{x}_j)\phi_{i,T}. \quad (3.15)$$

where the second term is added to deal with the jump of $u$ on the grid points, i.e., $w \neq 0$ on $\mathcal{N}_h^s$,

Then we define the interpolation of $u$ as

$$I_h u = \sum_{\mathbf{x}_i \in \mathcal{N}_h^i} u(\mathbf{x}_i)\phi_i + u_J, \quad (3.16)$$

and the nonhomogeneous IFE space $U_h(\Omega) = \text{span}\{\phi_j, j \in \mathcal{N}^i\} + u_J$. Then the numerical solution of (1.1)-(1.4) can be set as

$$u_h = \sum_{\mathbf{x}_i \in \mathcal{N}_h^i} U_i \phi_i + u_J \triangleq u_h^{hom} + u_J, \tag{3.17}$$

where $U_i$ is the uncertain coefficient to be solved by numerical methods, and $u_h^{hom} \in S_{h0}(\Omega)$ is the function satisfying homogeneous interface jump conditions and homogeneous boundary condition.

### 3.3 Immersed finite element methods

Non-conforming immersed finite element method (non-conforming IFEM) and Petrov-Galerkin immersed finite element method (PGIFEM) have been proposed in [11], [15] and [14], respectively. To describe these methods, we define $V_{h0}(\Omega)$ be the standard linear FE space with zero boundary. The nonhomogeneous IFE space $U_h(\Omega)$ is used as trial function space in both methods. For the non-conforming IFEM, $S_{h0}(\Omega)$ is used as test function space. Because that $S_{h0}(\Omega) \not\subseteq H_0^1(\Omega)$, the method has a consistent error and is called non-conforming IFEM. For the PGIFEM, $V_{h0}(\Omega)$ is used as test function space to cancel the consistent error because of $V_{h0}(\Omega) \subseteq H_0^1(\Omega)$. Then we have the following two numerical methods.

**Method 1** (Non-conforming IFEM). Find $u_h^{hom} \in S_{h0}(\Omega)$ such that

$$\begin{aligned} \sum_{T \in \mathcal{T}_h} \int_T \nabla u_h^{hom} \cdot \nabla v_h d\mathbf{x} = &- \sum_{T \in \mathcal{T}_h} \int_T \nabla u_J \cdot \nabla v_h d\mathbf{x} \\ &+ \int_\Omega f v_h d\mathbf{x} - \int_\Gamma Q v_h ds, \qquad \forall v_h \in S_{h0}(\Omega). \end{aligned} \tag{3.18}$$

**Method 2** (PGIFEM). Find $u_h^{hom} \in S_{h0}(\Omega)$ such that

$$\begin{aligned} \sum_{T \in \mathcal{T}_h} \int_T \nabla u_h^{hom} \cdot \nabla v_h d\mathbf{x} = &- \sum_{T \in \mathcal{T}_h} \int_T \nabla u_J \cdot \nabla v_h d\mathbf{x} \\ &+ \int_\Omega f v_h d\mathbf{x} - \int_\Gamma Q v_h ds, \qquad \forall v_h \in V_{h0}(\Omega). \end{aligned} \tag{3.19}$$

**Remark 3.2.**
*1. Non-conforming IFEM is symmetric, but not consistent, and numerical results in [11] indicate that the IFE solution does not have second order convergence in $L^\infty$ norm.*
*2. PGIFEM is consistent and has second order convergence in $L^\infty$ norm, but the resulting linear system of equations is nonsymmetric.*

Now we develop a symmetric and consistent immersed finite element method (SCIFEM). For

any subdomain $D = T \cap \Omega^+$ or $T \cap \Omega^-$, $T \in \mathcal{T}_h$, we have

$$\begin{aligned}\int_D f v_h d\mathbf{x} &= \int_D -\nabla(\beta \nabla u) v_h d\mathbf{x} \\ &= \int_D \beta \nabla u \cdot \nabla v_h d\mathbf{x} - \int_{\partial D} (\nabla u v_h) \cdot \mathbf{n} ds \qquad \forall v_h \in S_{h0}(\Omega).\end{aligned} \tag{3.20}$$

Let $e$ be an edge shared by two triangles $T_1$ and $T_2$, and $\mathbf{n}_i$ is the unit normal of $e$ pointing towards the outside of $T_i$, then the average and jump of $v$ are defined as

$$\{\!\{v\}\!\} = \frac{1}{2}(v|_{T_1} + v|_{T_2}), \qquad [\![v]\!]\mathbf{n}_1 = v|_{T_1}\mathbf{n}_1 + v|_{T_2}\mathbf{n}_2 = (v|_{T_1} - v|_{T_2})\mathbf{n}_1. \tag{3.21}$$

If $e$ is part of $\partial\Omega$, i.e., $e = \partial T \cap \partial\Omega$, we define $\{\!\{v\}\!\} = [\![v]\!] = v|_T$. Summing up (3.20) over all subdomains, we have

$$\begin{aligned}\int_\Omega f v_h d\mathbf{x} &= \sum_{T\in\mathcal{T}_h} \int_T \beta \nabla u \cdot \nabla v_h d\mathbf{x} - \sum_{e\in\mathcal{E}_h} \int_e [\![\beta \nabla u v_h]\!] \cdot \mathbf{n}_e ds - \int_\Gamma [\![\beta \nabla u v_h]\!] \cdot \mathbf{n} ds \\ &= \sum_{T\in\mathcal{T}_h} \int_T \beta \nabla u \cdot \nabla v_h d\mathbf{x} - \sum_{e\in\mathcal{E}_h} \int_e (\{\!\{\beta \nabla u\}\!\} [\![v_h]\!] + \{\!\{v_h\}\!\} [\![\beta \nabla u]\!]) \cdot \mathbf{n}_e ds \\ &\qquad - \int_\Gamma (\{\!\{\beta \nabla u\}\!\} [\![v_h]\!] + \{\!\{v_h\}\!\} [\![\beta \nabla u]\!]) \cdot \mathbf{n} ds \\ &= \sum_{T\in\mathcal{T}_h} \int_T \beta \nabla u \cdot \nabla v_h d\mathbf{x} - \sum_{e\in\mathcal{E}_h^{int}} \int_e \{\!\{\beta \nabla u\}\!\} [\![v_h]\!] \cdot \mathbf{n}_e ds + \int_\Gamma Q v_h ds,\end{aligned} \tag{3.22}$$

where the equality $[\![ab]\!] = \{\!\{a\}\!\}[\![b]\!] + \{\!\{b\}\!\}[\![a]\!]$ is used in the second equality, $[\![v_h]\!] = 0$ on $\Gamma$ and the jump condition (1.4) are used to derive the third term in the last equality, $[\![v_h]\!] = 0$ on $e \in \mathcal{E}_h^{non}$ and $[\![\beta \nabla u \cdot \mathbf{n}_e]\!] = 0$ on $e \in \mathcal{E}_h$ are used to derive the second term in the last equality. If we notice that $[\![u]\!] = 0$ on $e \in \mathcal{E}_h^{int} \backslash \partial\Omega$ and $[\![u]\!] = g$ on $e \in \mathcal{E}_h^{int} \cap \partial\Omega$, then we add the term $\sum_{e\in\mathcal{E}_h^{int}} \int_e \{\!\{\beta \nabla v_h\}\!\} \cdot \mathbf{n}_e [\![u]\!] ds$ to the above equation (3.22) for symmetric, then we have

$$\begin{aligned}&\sum_{T\in\mathcal{T}_h} \int_T \beta \nabla u \cdot \nabla v_h d\mathbf{x} - \sum_{e\in\mathcal{E}_h^{int}} \int_e (\{\!\{\beta \nabla u\}\!\} \cdot \mathbf{n}_e [\![v_h]\!] + \{\!\{\beta \nabla v_h\}\!\} \cdot \mathbf{n}_e [\![u]\!]) \, ds \\ &\qquad = \int_\Omega f v_h d\mathbf{x} - \int_\Gamma Q v_h ds - \sum_{e\in\mathcal{E}_h^{int}\cap\partial\Omega} \int_e \{\!\{\beta \nabla v_h\}\!\} \cdot \mathbf{n}_e g ds.\end{aligned} \tag{3.23}$$

If we use $U_h(\Omega)$ and $S_{h0}(\Omega)$ as trial and test function spaces respectively, then we have the following symmetric and consistent immersed finite element method.

**Method 3** (SCIFEM). Find $u_h^{hom} \in S_{h0}(\Omega)$ such that

$$\begin{aligned}
&\sum_{T\in\mathcal{T}_h}\int_T \nabla u_h^{hom}\cdot\nabla v_h d\mathbf{x} - \sum_{e\in\mathcal{E}_h^{int}}\int_e \left(\{\!\{\beta\nabla u_h^{hom}\}\!\}\cdot\mathbf{n}_e[\![v_h]\!] + \{\!\{\beta\nabla v_h\}\!\}\cdot\mathbf{n}_e[\![u_h^{hom}]\!]\right) ds \\
&\quad = -\sum_{T\in\mathcal{T}_h}\int_T \nabla u_J\cdot\nabla v_h d\mathbf{x} + \sum_{e\in\mathcal{E}_h^{int}}\int_e (\{\!\{\beta\nabla u_J\}\!\}\cdot\mathbf{n}_e[\![v_h]\!] + \{\!\{\beta\nabla v_h\}\!\}\cdot\mathbf{n}_e[\![u_J]\!])\, ds \qquad (3.24)\\
&\qquad - \sum_{e\in\mathcal{E}_h^{int}\cap\partial\Omega}\int_e \{\!\{\beta\nabla v_h\}\!\}\cdot\mathbf{n}_e g ds + \int_\Omega f v_h d\mathbf{x} - \int_\Gamma Q v_h ds, \qquad \forall v_h \in S_{h0}(\Omega).
\end{aligned}$$

**Remark 3.3.**
*1. Obviously, the resulting linear system of equations is symmetric. Furthermore, we note that the coefficient matrix is exactly the same as that in the SCIFEM for homogeneous jump conditions discussed in [16], then the coefficient matrix is also positive define.*
*2. When the discontinuity of $\beta$ disappears and $w = 0$, $Q = 0$, it becomes the standard P1 conforming finite element method.*
*3. Moreover, it need not a lot of time to deal with the corrections on $\mathcal{E}_h^{int}$ because that the corrections are added near the interface.*

# 4 Numerical experiments

In this section, we present some numerical examples to show the performance of the methods introduced in this paper. For simplicity, we solve the problem (1.1)-(1.4) in the rectangular domain $\Omega = [-1, 1] \times [-1, 1]$ with given analytic solution $u^+(\mathbf{x})$, $u^-(\mathbf{x})$, $\beta^+(\mathbf{x})$, $\beta^-(\mathbf{x})$ and the level set function $\varphi(\mathbf{x})$. Then $f$, $g$, $w$ and $Q$ are determined. In this section, we use $\mathbf{x} = (x, y)$ instead of $(x_1, x_2)$ for simplicity. The domain is partitioned into $2N^2$ right triangles with mesh size $h$.

The interface may hit grid points and $[u] = w \neq 0$, which cause two different values of these points, see Remark 3.1. We restrict these values of these points on $\Omega^-$ and set $\varphi(\mathbf{x}) = 0$, if $|\varphi(\mathbf{x})| < \epsilon$ ($\epsilon$ =1.0E-14) to avoid the ambiguity caused by $\varphi(\mathbf{x})$ smaller than machine precision.

In evaluating the integrals related norms and right hands, we divide an interface element into three small triangles and then use the three-point Gaussian quadrature formulae on each small triangle. For non-interface elements, the three-point Gaussian quadrature is used directly.

Define piecewise linear function $Q_h$ on $\Gamma_h$ such that $Q_h(\mathbf{x}^i) = Q(\mathbf{x}^i)$, where $\mathbf{x}^i$ is the intersections of the interface and edges of elements. Since the interface $\Gamma$ is approximated by $\Gamma_h$, see (3.2), the term $\int_\Gamma Q v_h ds$ in all above numerical methods is evaluated approximatively by $\int_{\Gamma_h} Q_h v_h ds$.

Errors in $L^\infty$ norm are computed approximately by

$$\|u - u_h\|_{L^\infty} = \max_{p\in\mathcal{N}_h} |u(p) - u_h(p)|,$$

and errors in broken $H^1$ norm are computed by

$$|u-u_h|_{H^1(\Omega)} = \sum_{T\in\mathcal{T}_h} (|u-u_h|_{H^1(T\cap\Omega^+)} + |u-u_h|_{H^1(T\cap\Omega^-)}),$$

where the notation $|u-u_h|_{H^1(\Omega)}$ is only used for simplicity although $u \notin H^1(\Omega)$. It is known for interface problems that the error does not necessarily behave monotonically under mesh refinement. Therefore, the asymptotic convergence order is usually defined as the slope of the linear least square fit of the error over mesh size in a log-log diagram. In the following examples, we plot errors in three norms in log-log scale on 31 different meshes ranging from $N = 2^3$ to $N = 2^{10}$. For example, we set $N_i = \mathit{floor}(2^{3+\frac{7}{30}(i-1)})$, for the $i$-th mesh, $1 \le i \le 31$, where the function $\mathit{floor}(k)$ rounds $k$ to the nearest integers less than or equal to $k$. The asymptotic convergence orders are the slopes $s$ of the linear least square fit of the errors on the 15 finest meshes because that coarsest meshes maybe resolve the interface poorly.

**Example 1.** This example is taken from [14]. The analytic solution $u^{\pm}$, the coefficients $\beta^{\pm}$ and level set function $\varphi$ are given as follows:

$$\begin{aligned} &u^+ = \ln(x^2+y^2), && u^- = \sin(x+y),\\ &\beta^+ = \sin(x+y)+2, && \beta^- = \cos(x+y)+2,\\ &\varphi = x^2+y^2-0.5^2. \end{aligned}$$

The interface is a simple circle with radius 0.5 and center at $(0,0)$. The set $\mathcal{N}^s$ is not empty, for example, $(0,0.5)$, $(0.3,0.4)$ and so on. Table 1 shows that the PGIFEM and the SCIFEM achieves second order accuracy in $L^\infty$ norm, but the non-conforming IFEM only has first order accuracy in $L^\infty$ norm. Figure 4 shows the numerical solution for Example 1 by SCIFEM with $N = 128$ and results of the linear regression analysis in three norms.

| | Non-conforming IFEM | | PGIFEM | | SCIFEM | |
|---|---|---|---|---|---|---|
| N | $\|u-u_h\|_{L^\infty}$ | Order | $\|u-u_h\|_{L^\infty}$ | Order | $\|u-u_h\|_{L^\infty}$ | Order |
| 64 | 0.14893E-02 | | 0.53439E-03 | | 0.89247E-03 | |
| 128 | 0.60514E-03 | 1.29927 | 0.16957E-03 | 1.65604 | 0.22597E-03 | 1.98170 |
| 256 | 0.27970E-03 | 1.11340 | 0.44741E-04 | 1.92217 | 0.56830E-04 | 1.99138 |
| 512 | 0.14894E-03 | 0.90911 | 0.11443E-04 | 1.96716 | 0.14217E-04 | 1.99902 |
| 1024 | 0.74133E-04 | 1.00657 | 0.29100E-05 | 1.97534 | 0.35880E-05 | 1.98636 |

Table 1: compare of the convergence results for Example 1 in $L^\infty$ norm by three methods.

**Example 2.** This example is taken from [14]. The analytic solution $u^{\pm}$, the coefficients $\beta^{\pm}$ and level set function $\varphi$ are given as follows:

$$\begin{aligned} &u^+ = 1-x^2-y^2, && u^- = x^2+y^2+2,\\ &\beta^+ = x^2-y^2+3, && \beta^- = 1000(xy+3),\\ &\varphi = x^2+y^2-0.5^2. \end{aligned}$$

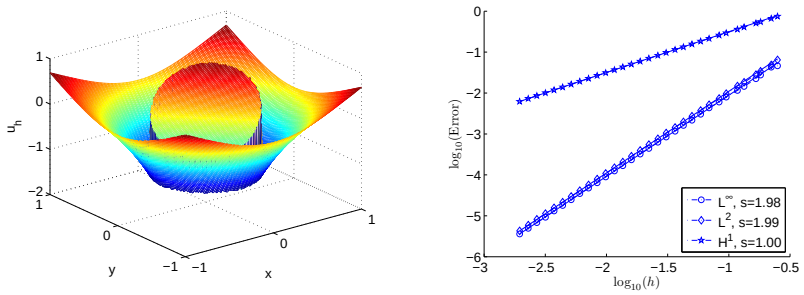


Figure 4: Solution for Example 1 solved by SCIFEM with $N = 128$ (left) and the linear regression analysis in three norms in log-log scale (right).

The difficulty of the example is that $\beta^+/\beta^- \approx 1/1000$. The results are reported in Table 2 and Figure 5. From Table 2, we find that the error constant in $L^\infty$ norm of SCIFEM is much smaller that that of PGIFEM although they both have second order accuracy, and the non-conforming IFEM also only has nearly first order accuracy in $L^\infty$ norm.

| | Non-conforming IFEM | | PGIFEM | | SCIFEM | |
|---|---|---|---|---|---|---|
| N | $\|u-u_h\|_{L^\infty}$ | Order | $\|u-u_h\|_{L^\infty}$ | Order | $\|u-u_h\|_{L^\infty}$ | Order |
| 64 | 0.19181E+00 | | 0.28255E+00 | | 0.10346E+00 | |
| 128 | 0.85401E-01 | 1.16732 | 0.71235E-01 | 1.98785 | 0.30468E-01 | 1.76366 |
| 256 | 0.52817E-01 | 0.69325 | 0.17731E-01 | 2.00627 | 0.74824E-02 | 2.02574 |
| 512 | 0.17012E-01 | 1.63449 | 0.44679E-02 | 1.98863 | 0.19830E-02 | 1.91580 |
| 1024 | 0.98813E-02 | 0.78374 | 0.10857E-02 | 2.04102 | 0.48505E-03 | 2.03149 |

Table 2: Compare of the convergence results for Example 2 in $L^\infty$ norm by three methods.

**Example 3.** The analytic solution $u^\pm$, the coefficients $\beta^\pm$ and level set function $\varphi$ are given as follows:

$$\begin{aligned} u^+ &= 5 - 5x^2 - 5y^2, & u^- &= 7x^2 + 7y^2 + 6, \\ \beta^+ &= (xy+2)/5, & \beta^- &= (x^2 - y^2 + 3)/7, \\ \varphi &= r - (0.5 + 0.1\sin(5\theta)), \end{aligned}$$

where $(r, \theta)$ is the polar coordinate of $(x, y)$. The difficulty of this example is that the interface has complicated geometry. Similar results are reported in Table 3 and Figure 6. From the picture, we see that the order of SCIFEM in $L^\infty$ is 2.13 when the mesh resolved the complicated interface.

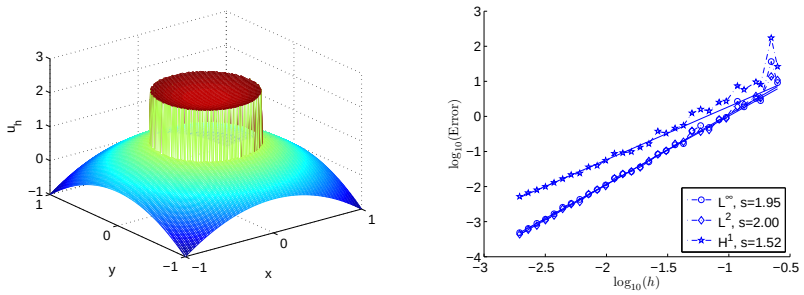


Figure 5: Solution for Example 2 solved by SCIFEM with $N = 128$ (left) and the linear regression analysis in three norms in log-log scale (right).

| | Non-conforming IFEM | | PGIFEM | | SCIFEM | |
|---|---|---|---|---|---|---|
| N | $\|u - u_h\|_{L^\infty}$ | Order | $\|u - u_h\|_{L^\infty}$ | Order | $\|u - u_h\|_{L^\infty}$ | Order |
| 64 | 0.70391E-02 | | 0.69993E-02 | | 0.78501E-02 | |
| 128 | 0.10552E-02 | 2.73782 | 0.10545E-02 | 2.73072 | 0.14928E-02 | 2.39468 |
| 256 | 0.35071E-03 | 1.58923 | 0.34386E-03 | 1.61661 | 0.41616E-03 | 1.84283 |
| 512 | 0.97224E-04 | 1.85088 | 0.95652E-04 | 1.84595 | 0.12020E-03 | 1.79167 |
| 1024 | 0.59412E-04 | 0.71055 | 0.20257E-04 | 2.23937 | 0.21450E-04 | 2.48641 |

Table 3: Compare of the convergence results for Example 3 in $L^\infty$ norm by three methods.

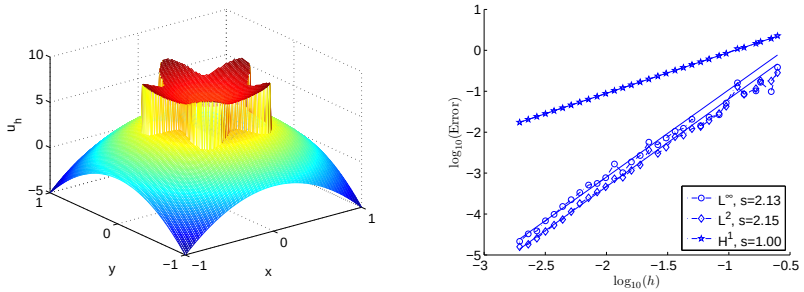


Figure 6: Solution for Example 3 solved by SCIFEM with $N = 128$ (left) and the linear regression analysis in three norms in log-log scale (right).

**Example 4.** This example is taken from [19]. The analytic solution $u^{\pm}$, the coefficients $\beta^{\pm}$ and

level set function $\varphi$ are given as follows:

$$u^+ = \frac{r^4 - C_0 \log(2r)}{\beta^+}, \qquad u^- = \frac{r^2}{\beta^-},$$
$$\beta^+ = \text{const.}, \qquad \beta^- = \text{const.},$$
$$\varphi = \sqrt{(x-x_c)^2 + (y-y_c)^2} - (r_0 + r_1 \sin(\omega\theta)),$$

where $(r, \theta)$ is the polar coordinate of $(x, y)$, $C_0 = -0.1$, $(x_c, y_c) = (0.2/\sqrt{20}, 0.2/\sqrt{20})$, $r_0 = 0.5$, $r_1 = 0.2$, $\omega = 5$ and $\beta^{\pm}$ are positive constants. We provide numerical results for three typical cases. *Case 1* (moderate jump): $\beta^+ = 10$, $\beta^- = 1$. *Case 2* (large jump): $\beta^+ = 1000$, $\beta^- = 1$. *Case 3* (large jump): $\beta^+ = 1$, $\beta^- = 1000$. The results are reported in Table 4-6 and Figure 7-9.

| | Non-conforming IFEM | | PGIFEM | | SCIFEM | |
|---|---|---|---|---|---|---|
| N | $\|u-u_h\|_{L^\infty}$ | Order | $\|u-u_h\|_{L^\infty}$ | Order | $\|u-u_h\|_{L^\infty}$ | Order |
| 64 | 0.23951E-02 | | 0.96132E-03 | | 0.90778E-03 | |
| 128 | 0.10078E-02 | 1.24883 | 0.17549E-03 | 2.45365 | 0.13393E-03 | 2.76091 |
| 256 | 0.72664E-03 | 0.47192 | 0.47604E-04 | 1.88221 | 0.38253E-04 | 1.80778 |
| 512 | 0.38903E-03 | 0.90134 | 0.16422E-04 | 1.53548 | 0.17286E-04 | 1.14602 |
| 1024 | 0.19958E-03 | 0.96294 | 0.31922E-05 | 2.36302 | 0.30992E-05 | 2.47961 |

Table 4: Compare of the convergence results for Example 4 case 1 in $L^\infty$ norm by three methods.

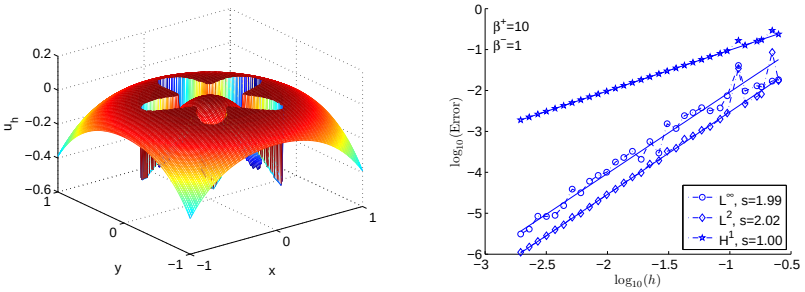


Figure 7: Solution $-u_h$ for Example 4 case 1 solved by SCIFEM with $N = 128$ (left) and the linear regression analysis in three norms in log-log scale (right).

| | Non-conforming IFEM | | PGIFEM | | SCIFEM | |
|---|---|---|---|---|---|---|
| N | $\|u-u_h\|_{L^\infty}$ | Order | $\|u-u_h\|_{L^\infty}$ | Order | $\|u-u_h\|_{L^\infty}$ | Order |
| 64 | 0.20093E-02 | | 0.32980E-02 | | 0.81674E-03 | |
| 128 | 0.46009E-03 | 2.12671 | 0.54701E-03 | 2.59194 | 0.19840E-03 | 2.04144 |
| 256 | 0.21123E-03 | 1.12312 | 0.23527E-03 | 1.21726 | 0.72054E-04 | 1.46128 |
| 512 | 0.78331E-04 | 1.43114 | 0.68935E-04 | 1.77101 | 0.20948E-04 | 1.78228 |
| 1024 | 0.37179E-04 | 1.07510 | 0.15269E-04 | 2.17466 | 0.11668E-05 | 4.16620 |

Table 5: Compare of the convergence results for Example 4 case 2 in $L^\infty$ norm by three methods.

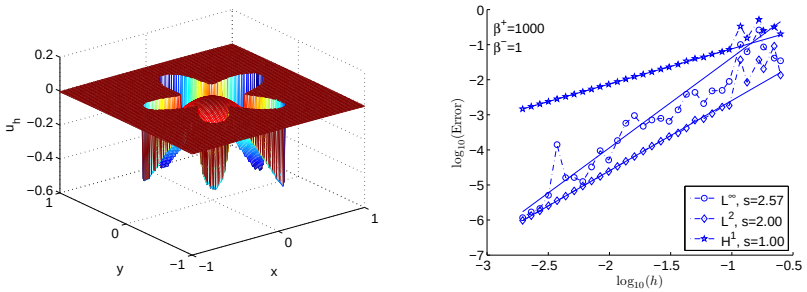


Figure 8: Solution $-u_h$ for Example 4 case 2 solved by SCIFEM with $N = 128$ (left) and the linear regression analysis in three norms in log-log scale (right).

| | Non-conforming IFEM | | PGIFEM | | SCIFEM | |
|---|---|---|---|---|---|---|
| N | $\|u-u_h\|_{L^\infty}$ | Order | $\|u-u_h\|_{L^\infty}$ | Order | $\|u-u_h\|_{L^\infty}$ | Order |
| 64 | 0.57000E-02 | | 0.57055E-02 | | 0.44289E-02 | |
| 128 | 0.19265E-02 | 1.56501 | 0.20804E-02 | 1.45553 | 0.94519E-03 | 2.22828 |
| 256 | 0.67517E-03 | 1.51262 | 0.70046E-03 | 1.57045 | 0.72597E-04 | 3.70262 |
| 512 | 0.17765E-03 | 1.92620 | 0.17819E-03 | 1.97488 | 0.69692E-04 | 0.05892 |
| 1024 | 0.56174E-04 | 1.66110 | 0.30348E-04 | 2.55375 | 0.28918E-05 | 4.59097 |

Table 6: Compare of the convergence results for Example 4 case 3 in $L^\infty$ norm by three methods.

**Example 5.** This example is taken from [14]. The analytic solution $u^\pm$, the coefficients $\beta^\pm$ and level set function $\varphi$ are given as follows:

$$u^+ = 4 - x^2 - y^2, \qquad u^- = x^2 + y^2,$$
$$\beta^+ = xy + 2, \qquad \beta^- = x^2 - y^2 + 3,$$
$$\varphi = x^2 - y - 1.$$

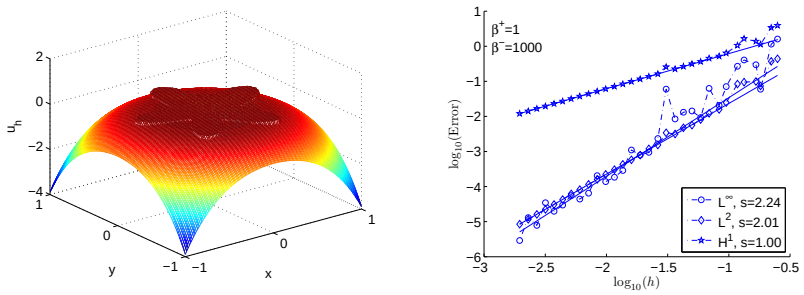


Figure 9: Solution $-u_h$ for Example 4 case 3 solved by SCIFEM with $N = 128$ (left) and the linear regression analysis in three norms in log-log scale (right).

The interface is tangential to the boundary $\partial\Omega$ at $(0, -1)$, and it intersects with the boundary $\partial\Omega$ at $(-1, 0)$ and $(1, 0)$ at certain nonzero angles. The results are reported in Table 7 and Figure 10.

| | Non-conforming IFEM | | PGIFEM | | SCIFEM | |
|---|---|---|---|---|---|---|
| N | $\|u - u_h\|_{L^\infty}$ | Order | $\|u - u_h\|_{L^\infty}$ | Order | $\|u - u_h\|_{L^\infty}$ | Order |
| 64 | 0.86962E-03 | | 0.18257E-03 | | 0.29018E-03 | |
| 128 | 0.49958E-03 | 0.79966 | 0.46145E-04 | 1.98421 | 0.77109E-04 | 1.91197 |
| 256 | 0.26691E-03 | 0.90438 | 0.12095E-04 | 1.93183 | 0.20634E-04 | 1.90185 |
| 512 | 0.14432E-03 | 0.88712 | 0.30143E-05 | 2.00446 | 0.51842E-05 | 1.99287 |
| 1024 | 0.75154E-04 | 0.94130 | 0.76066E-06 | 1.98649 | 0.13548E-05 | 1.93602 |

Table 7: Compare of the convergence results for Example 5 in $L^\infty$ norm by three methods.

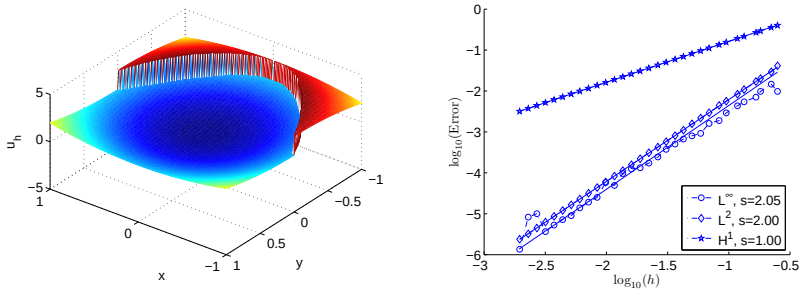


Figure 10: Solution for Example 5 solved by SCIFEM with $N = 128$ (left) and the linear regression analysis in three norms in log-log scale (right).

**Example 6.** This example is taken from [22, p. 50, Example 3.2]. The analytic solution $u^{\pm}$, the

coefficients $\beta^{\pm}$ and level set function $\varphi$ are given as follows:

$$\begin{aligned} u^+ &= \sin(2x)\cos(2y), & u^- &= (2x)^2 - (2y)^2, \\ \beta^+ &= 10, & \beta^- &= 1, \\ \varphi &= x^2 + (2y)^2 - 0.5^2. \end{aligned}$$

The results are reported in Table 8 and Figure 11.

| | Non-conforming IFEM | | PGIFEM | | SCIFEM | |
|---|---|---|---|---|---|---|
| N | $\|u-u_h\|_{L^\infty}$ | Order | $\|u-u_h\|_{L^\infty}$ | Order | $\|u-u_h\|_{L^\infty}$ | Order |
| 64 | 0.11712E-01 | | 0.31748E-02 | | 0.11800E-02 | |
| 128 | 0.57292E-02 | 1.03153 | 0.88727E-03 | 1.83921 | 0.29410E-03 | 2.00437 |
| 256 | 0.32554E-02 | 0.81550 | 0.25454E-03 | 1.80148 | 0.62505E-04 | 2.23425 |
| 512 | 0.15209E-02 | 1.09794 | 0.61939E-04 | 2.03897 | 0.17074E-04 | 1.87219 |
| 1024 | 0.86572E-03 | 0.81295 | 0.15939E-04 | 1.95829 | 0.35861E-05 | 2.25127 |

Table 8: Compare of the convergence results for Example 6 in $L^\infty$ norm by three methods.

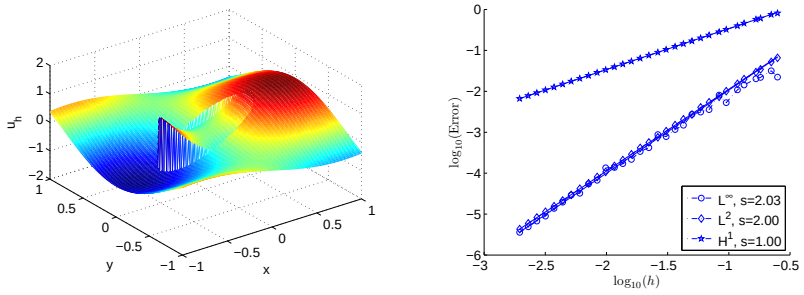


Figure 11: Solution for Example 6 solved by SCIFEM with $N = 128$ (left) and the linear regression analysis in three norms in log-log scale (right).

**Example 7.** This example is taken from [14]. The analytic solution $u^{\pm}$, the coefficients $\beta^{\pm}$ and level set function $\varphi$ are given as follows:

$$\begin{aligned} u^+ &= 1 - x^2 - y^2, & u^- &= x^2 + y^2 + 2, \\ \beta^+ &= x^2 - y^2 + 3, & \beta^- &= xy + 3, \\ \varphi &= (3(x^2+y^2) - x)^2 - x^2 - y^2. \end{aligned}$$

The specific feature of this example is the singular point of the interface with a cusp point at $(0, 0)$. The results are reported in Table 9 and Figure 12.

| | Non-conforming IFEM | | PGIFEM | | SCIFEM | |
|---|---|---|---|---|---|---|
| N | $\|u-u_h\|_{L^\infty}$ | Order | $\|u-u_h\|_{L^\infty}$ | Order | $\|u-u_h\|_{L^\infty}$ | Order |
| 64 | 0.92622E-03 | | 0.92845E-03 | | 0.87632E-03 | |
| 128 | 0.30335E-03 | 1.61039 | 0.30352E-03 | 1.61303 | 0.28133E-03 | 1.63917 |
| 256 | 0.66835E-04 | 2.18229 | 0.66891E-04 | 2.18191 | 0.66515E-04 | 2.08053 |
| 512 | 0.16286E-04 | 2.03699 | 0.16298E-04 | 2.03713 | 0.16210E-04 | 2.03680 |
| 1024 | 0.57653E-05 | 1.49814 | 0.38885E-05 | 2.06742 | 0.39384E-05 | 2.04121 |

Table 9: Compare of the convergence results for Example 7 in $L^\infty$ norm by three methods.

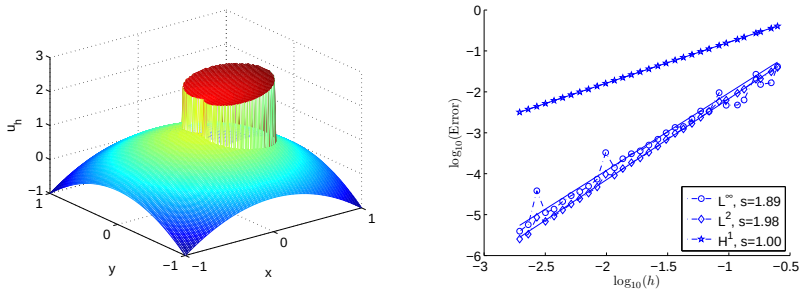


Figure 12: Solution for Example 7 solved by SCIFEM with $N = 128$ (left) and the linear regression analysis in three norms in log-log scale (right).

# 5 Conclusions

We have developed a new symmetric and consistent immersed finite element method (SCIFEM) for solving elliptic interface problems with nonhomogeneous jump conditions on structured meshes. The interface may intersect with $\partial\Omega$ and grid points. The new SCIFEM has optimal convergence rates in the $H^1$, $L^2$, and $L^\infty$ norms which are verified numerically.

## Acknowledgments

This work was supported in part by NSFC grant 11071124 and 11226334, the Program of Natural Science Research of Jiangsu Higher Education Institutions of China (Grant No. 12KJB110013), and the Innovation Project for Graduate Education of Jiangsu Province (CXLX13_365).

# References


[1] J. Bramble and J. King. A finite element method for interface problems in domains with smooth boundaries and interfaces. *Advances in Comput. Math.*, 6:109–138, 1996.

[2] B. Camp, T. Lin, Y. Lin, and W. Sun. Quadratic immersed finite element spaces and their approximation capabilities. *Adv. Comput. Math.*, 24:81–112, 2006.

[3] K. S. Chang and D. Y. Kwak. Discontinuous bubble scheme for elliptic problems with jumps in the solution. *Comput Methods Appl. Mech. Engrg*, 200:494–508, 2011.

[4] Z. Chen and J. Zou. Finite element methods and their convergence for elliptic and parabolic interface problems. *Numer. Math.*, 79:175–202, 1998.

[5] S. Chou, D. Kwak, and K. Wee. Optimal convergence analysis of an immersed interface finite element method. *Adv. Comput. Math.*, 33:149–168, 2010.

[6] M. Discacciati, A. Quarteroni, and S. Quinodoz. Numerical approximation of internal discontinuity interface problems. *SIAM J. Sci. Comput.*, 35:A2341–A2369, 2013.

[7] T. Fries and T. Belytschko. The extended/generalized finite element method: an overview of the method and its applications. *Internat. J. Numer. Methods in Engrg.*, 84:253–304, 2010.

[8] Y. Gong, B. Li, and Z. Li. Immersed-interface finite-element methods for elliptic interface problems with non-homogeneous jump conditions. *SIAM J. Numer. Anal.*, 46:472–495, 2008.

[9] A. Hansbo and P. Hansbo. An unfitted finite element method, based on Nitsche's method, for elliptic interface problems. *Comput. Methods Appl. Mech. Engrg.*, 191:5537–5552, 2002.

[10] X. He, T. Lin, and Y. Lin. Approximation capability of a bilinear immersed finite element space. *Numer. Methods Partial Differential Equations*, 24:1265–1300, 2008.

[11] X. He, T. Lin, and Y. Lin. Immersed finite element methods for elliptic interface problems with non-homogeneous jump conditions. *Int. J. Numer. Anal. Model.*, 8:284–301, 2011.

[12] X. He, T. Lin, and Y. Lin. The convergence of the bilinear and linear immersed finite element solutions to interface problems. *Numer. Methods Partial Differential Equations*, 28:312–330, 2012.

[13] S. Hou, Z. Li, L. Wang, and W. Wang. A numerical method for solving elasticity equations with interfaces. *Commun. Comput. Phys.*, 12:595, 2012.

[14] S. Hou and X. Liu. A numerical method for solving variable coefficient elliptic equation with interfaces. *J. Comput. Phys.*, 202:411–445, 2005.

[15] T. Hou, X. Wu, and Y. Zhang. Removing the cell resonance error in the multiscale finite element method via a Petrov-Galerkin formulation. *Comm. Math. Sci*, 2:185–205, 2004.

[16] H. Ji, J. Chen, and Z. Li. A symmetric and consistent immersed finite element method for interface problems. *submitted*.

[17] D. Kwak, K. Wee, and K. Chang. An analysis of a broken $P_1$-nonconforming finite element method for interface problems. *SIAM J. Numer. Anal.*, 48:2117–2134, 2010.

[18] R. Leveque and Z. Li. The immersed interface method for elliptic equations with discontinuous coefficients and singular sources. *SIAM J. Numer. Anal.*, 31:1019–1044, 1994.

[19] Z. Li. A fast iterative algorithm for elliptic interface problems. *SIAM J. Numer. Anal*, 35:230–254, 1998.

[20] Z. Li. The immersed interface method using a finite element formulation. *Appl. Numer. Math.*, 27:253–267, 1998.

[21] Z. Li and K. Ito. Maximum principle preserving schemes for interface problems with discontinuous coefficients. *SIAM J. Sci. Comput.*, 23:1225–1242, 2001.

[22] Z. Li and K. Ito. *The immersed interface method: numerical solutions of PDEs involving interfaces and irregular domains*, volume 33. siam, 2006.

[23] Z. Li, T. Lin, Y. Lin, and R. Rogers. An immersed finite element space and its approximation capability. *Numer. Methods Partial Differential Equations*, 20:338–367, 2004.

[24] Z. Li, T. Lin, and X. Wu. New cartesian grid methods for interface problems using the finite element formulation. *Numer. Math.*, 96:61–98, 2003.

[25] T. Lin, Y. Lin, R. Rogers, and M. Ryan. A rectangular immersed finite element space for interface problems. *Advances in computation: theory and practice*, 7:107–114, 2001.

[26] T. Lin, Y. Lin, and W. Sun. Error estimation of a class of quadratic immersed finite element methods for elliptic interface problems. *Discrete Contin. Dyn. Syst. Ser. B*, 7:807, 2007.

[27] T. Lin and X. Zhang. Linear and bilinear immersed finite elements for planar elasticity interface problems. *J. Comput. Appl. Math.*, 236:4681–4699, 2012.

[28] R. Massjung. An unfitted discontinuous galerkin method applied to elliptic interface problems. *SIAM J. Numer. Anal.*, 50:3134–3162, 2012.

[29] M. Oevermann and R. Klein. A cartesian grid finite volume method for elliptic equations with variable coefficients and embedded interfaces. *J. Comput. Phys*, 219:749–769, 2006.

[30] M. Oevermann, C. Scharfenberg, and R. Klein. A sharp interface finite volume method for elliptic equations on cartesian grids. *J. Comput. Phys.*, 228:5184–5206, 2009.

[31] J. Xu. Error estimates of the finite element method for the 2nd order elliptic equations with discontinuous coefficients. *J. Xiangtan University*, 1:1–5, 1982.

[32] X. Yang, B. Li, and Z. Li. The immersed interface method for elasticity problems with interface. *Dyn. Contin. Discrete Impuls. Syst. Ser. A Math. Anal.*, 10:783–808, 2003.

[33] S. Yu, Y. Zhou, and G. Wei. Matched interface and boundary (MIB) method for elliptic problems with sharp-edged interfaces. *J. Comput. Phys.*, 224:729–756, 2007.

[34] Y. Zhou, S. Zhao, M. Feig, and G. Wei. High order matched interface and boundary method for elliptic equations with discontinuous coefficients and singular sources. *J. Comput. Phys.*, 213:1–30, 2006.